Multifunctional integrated optical chip for fiber optical gyroscope fabricated by high temperature proton exchange

Yuri N. Korkishko*, Vyacheslav A. Fedorov, Sergey M. Kostritskii, Alexander N. Alkaev, Evgeny M.Paderin, Evgeny I.Maslennikov, Dmitry V.Apraksin

Optolink Ltd., Moscow Institute of Electronic Technology, PROTON, 124498, Moscow, Zelenograd, Russia.

ABSTRACT

Multifunctional integrated optical chip (MIOC) for fiber optical gyroscope with linear digital output is developed. The technology is based on recently proposed High-Temperature Proton Exchange method. MIOC is used for industrial closed-loop fiber optic gyro.

Keywords: multifunctional integrated optical chip, lithium niobate, fiber optical gyroscope.

I. INTRODUCTION

The fiber optical gyros (FOG) have a significant feature, being compared with the traditional spinning mass gyros [1], such as short worming-up time, light weight, maintenance free, reliability, wide dynamic range, large bandwidth and low power consumption.

One of the main fiber optical gyroscope's components is a multifunctional integrated optical chip (MIOC). Optolink's MIOC is a solid state waveguide device on X-cut $LiNbO_3$ substrate fabricated by High-Temperature Proton Exchange method (HTPE) [2]. It includes a linear polarizer, Y-junction coupler and two pairs of electro-optic phase modulators. Light coming from the optical fiber coupler is linearly polarized within the MIOC to greater than 60 dB. This high degree of polarization minimizes bias uncertainty due to polarization non-reciprocity. The Y-junction coupler within the MIOC splits the light into equal amplitude waves, each directed along a separate waveguide within the MIOC. Each of the resulting waves pass through a electrooptical phase modulator and after two waves counterpropagate around the optical PM optical fiber sensor coil. To achieve the low random walk and bias a 1070 m coil is used.

A very important advantage of proton exchange (PE) waveguides is following. In such waveguides the extraordinary refraction index is increasing, while refraction index of ordinary ray is decreasing. As a result, proton exchanged waveguides support propagation only extraordinary polarization modes (TE in our case). Therefore, it is no necessity to use in the fiber optical gyroscope a polarizer, which brings additional loss.

II. HIGH TEMPERATURE PROTON EXCHANGED WAVEGUIDES

It is well known, that standard technology of PE waveguide (APE-technology) [3] applies a two-level process, which consists of a PE, (melting pure or diluted by lithium benzoate benzoic acid as a rule) and subsequent annealing (Fig.1a). It was recently obtained, that different defects are formed in the surface area of waveguide due to different phase transitions [4]. These defects are sources of additional scattering of light.

* contact author: korkishko@optolink.ru; phone 7 095 536-9933; fax 7 095 536-9934; Optolink Ltd., Moscow Institute of Electronic Technology, Proton plant, 124498, Moscow, Zelenograd, Russia.

Integrated Optical Devices: Fabrication and Testing, Giancarlo C. Righini, Editor, Proceedings of SPIE Vol. 4944 (2003) © 2003 SPIE · 0277-786X/03/$15.00

In the paper [2] we reported the fabrication and characterization of $LiNbO_3$ optical waveguides prepared by HTPE process with a new proton exchange source, i.e., the mixture of stearic acid and lithium stearate. The melt used is characterized by the mass ratio of lithium stearate (LS) and stearic acid (SA): $\rho = m_{LS} / m_{SA}$. Varying ρ between 0 and 1% strongly modifies the phase of the exchanged layer. HTPE process, in contrast to APE (Fig.1a), is a one step process and does not allow any phase transitions (Fig.1b) for formation of α-phase PE $LiNbO_3$ waveguides, and, therefore, allows one to achieve the lower optical losses and higher electro-optical coefficients in the waveguides.

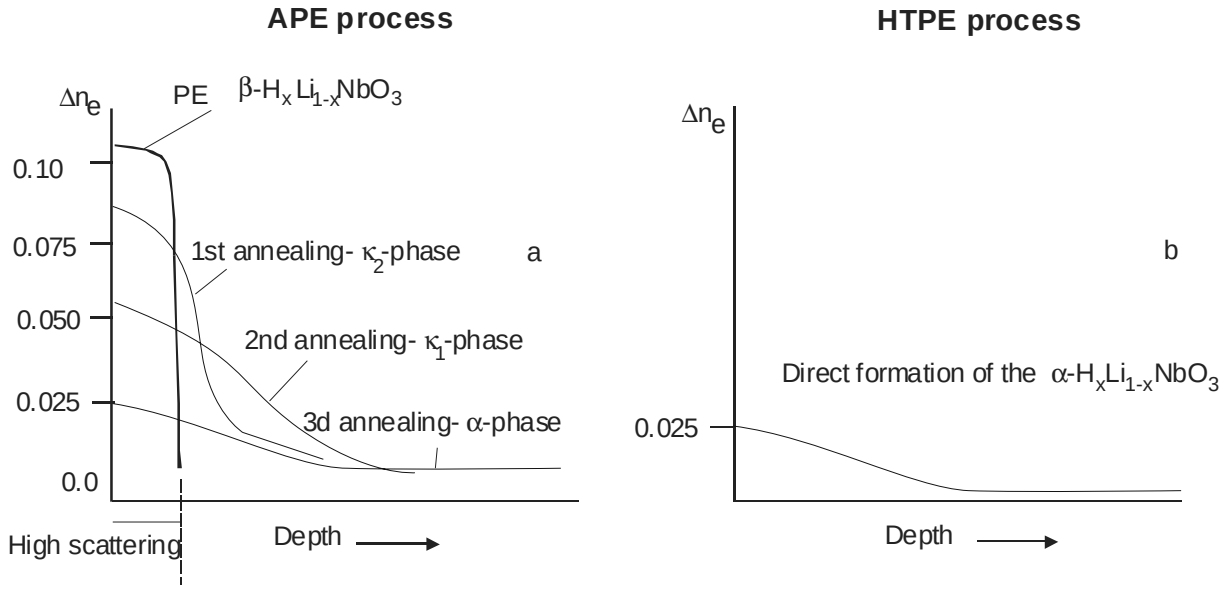

Fig.1. Formation of α-phase PE $LiNbO_3$ waveguides by APE (a) and HTPE (b) processes.

Fig.2 shows the variation of the $H_xLi_{1-x}NbO_3$ surface extraordinary refractive index increment, Δn_e, as a function of the LS content and temperature of the melt.

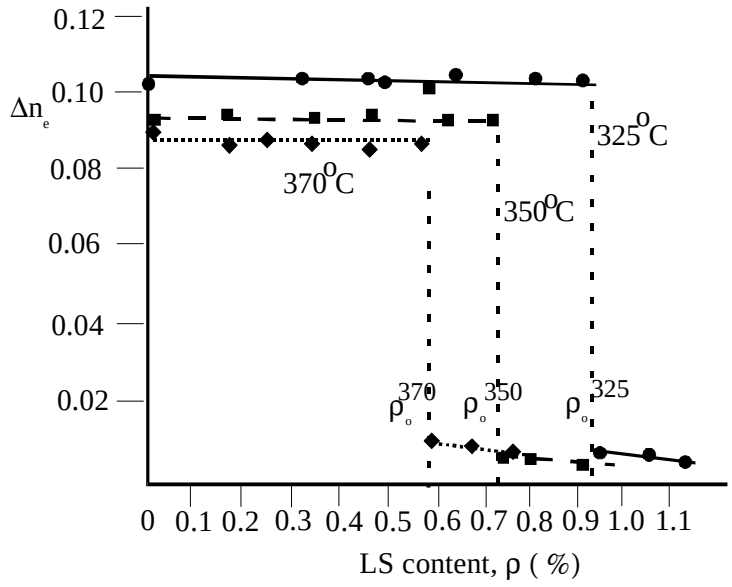

Fig.2. Surface index change, Δn_e, vs. composition of the melt, ρ, for different temperatures of HTPE.

With lithium stearate concentration higher than the threshold value, ρ_0, the Soft Proton Exchange process [5-7] is realized. In this case uniform α-phase waveguides are formed, which present graded index profiles with a maximum index increase Δn_α^o=0.02 at 830 nm wavelength.

The HTPE processes are carried out in the specially developed containers [2].

The specially developed metal and dielectric films are used as masks to provide local proton exchange diffusion. Then by vacuum deposition of electrodes, the integrated electro-optical phase modulators are formed on both arms of Y-splitter. After the end surfaces are cut (the angle is 10 degree to the Z axis), polished, and finally they are coupled with input isotropic and two output anisotropic polarization holding (PANDA) fibers by using EXFO automatic aligner F-3000. The final steps are packaging and welding of electrodes.

III. SIMULATION OF MIOC

The proton exchange diffusion kinetics in *x*-direction is governed by the nonlinear equation [8,9]:

$$\frac{\partial C^H(x,z,t)}{\partial t} = \frac{\partial}{\partial x}\left(D_x(x,z)\frac{\partial C}{\partial x}\right) + \frac{\partial}{\partial z}\left(D_z(x,z)\frac{\partial C}{\partial z}\right) \qquad (1)$$

where $C^H(x,z,t)$ is proton concentration, $D_x(x,z)$ and $D_z(x,z)$ are interdiffusion coefficients in x- and z-directions, respectively. These coefficients can be obtained from known self-diffusion coefficients of protons, D_x^H and D_z^H and lithium ions, D_x^{Li} and D_z^{Li} as following [9]:

$$D_x(x,z) = \frac{D_x^H}{1 - C_{x,z}\alpha_x}$$
$$D_z(x,z) = \frac{D_z^H}{1 - C_{x,z}\alpha_z} \qquad (2)$$

where α_x and α_z are:

$$\alpha_x = 1 - \frac{D_x^H}{D_x^{Li}} \text{ and } \alpha_z = 1 - \frac{D_z^H}{D_z^{Li}} \qquad (3)$$

The temperature dependence of self-diffusion coefficients of protons and lithium ions follows the Arrhenius law,

$$D_{x,z}^H = D_{x,z}^{H0}\exp\left(-\frac{Q_{x,z}^H}{RT}\right)$$
$$D_{x,z}^{Li} = D_{x,z}^{Li0}\exp\left(-\frac{Q_{x,z}^{Li}}{RT}\right) \qquad (4)$$

where $D_{x,z}^{H0}$, $D_{x,z}^{Li0}$ are diffusion constants for protons and lithium ions, respectively, $Q_{x,z}^H$ and $Q_{x,z}^H$ are their activation energies and *R* is an universal gas constant.

In ref. [10] the following diffusion parameters for X-cut $LiNbO_3$ were obtained: D_x^{H0}=2.3x10^7 μm^2/h, Q_x^H =84.5 kJ/mol and D_x^{Li0}=1.9x10^{11} μm^2/h, Q_x^{Li} =130.6 kJ/mol. Unfortunately, these values for Z-cut are still unknown.

However, the diffusion rates for SPE processes at X- and Z-cut of $LiNbO_3$ are relatively closed, and in our calculations we assumed that $D_x^{H0} \approx D_z^{H0}$, $Q_x^H \approx Q_z^H$, $D_x^{Li0} \approx D_z^{Li0}$ and $Q_x^{Li} \approx Q_z^{Li}$.

Fig. 3 shows the results of calculations of proton distribution for one cross-section of Y-branch region. Results presented for two waveguides with width w_1=4 μm and separated at w_2=10 μm. The dependence of proton concentration on extraordinary index change is known [11]. For α-phase $H_xLi_{1-x}NbO_3$ $C^H=4.8\cdot\Delta n_e$ and, therefore, the distribution of index change can be calculated for all region of Y-splitter.

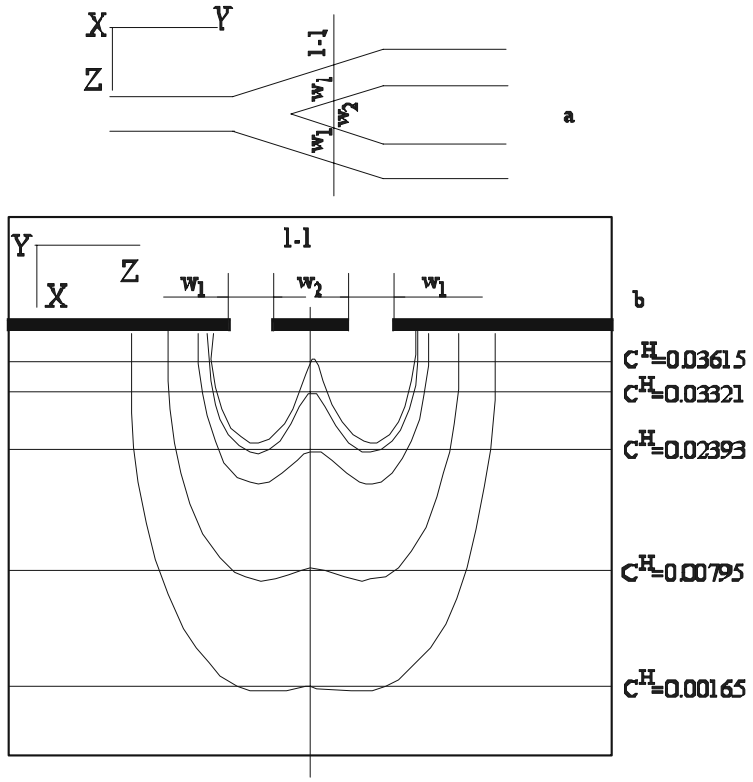

Fig. 3. The view of Y-splitter (a) and proton distribution in one cross-section (b).

After that we know index distribution in structure, the beam propagation method (BPM) [12] is used for simulation of light propagation in Y-splitter. The results of simulations are close to experimentally obtained.

IV. DEVICE PERFORMANCE

MIOC is a monoblock hermetic product, which is connected to the optical block of FOG by means of fiber waveguide splicing and soldering phase modulator electrical outputs to the electronic blocks.

Main parameters of OPTOLINK MIOC with operating wavelength 830±30 nm are following:

- optical power losses (at depolarized light), dB	< 7;
- polarizer extinction ratio, dB	> 60;
- splitting ratio	0,5± 0,05;
- phase sensitivity of each modulator, rad/V	> 1

MIOC is a key element of OPTOLINK's fiber optical gyro. The general block diagram of the device developed and manufactured is shown on the Fig.4. The two counterpropagating waves traversing the coil recombine at the Y-junction

of the MIOC. The interference results in a rotation rate-dependent intensity which propagates to the 2x2 fiber coupler (beam splitter) and then to the photodetector. A closed loop modulation scheme based on all digital serrodyne technique is used in our FOG. It means a $\pi/2$ phase shift is imposed upon one of the counterpropagating waves relative to the other as well as Sangac phase shift is compensated. In this case the control signal of the phase modulator can be used to measure the rotation rate. It is well known that at such approach output characteristic of FOG is linear and scale factor is independent from parameters of almost all components of the device. This is very important because if we process the information by means of a variable signal or a digital method, then along with the stability improvement of scale coefficient the number of the electronic factors which have an influence on the output signal error is essentially reduced.

FOG's sensitivity to the rotation is mainly determined by the fiber loop design, its size, fiber type, and the wounding method. The single-mode polarization maintaining optical fiber (PANDA) with strong birefringence is used. Present technology level of fiber manufacturing on the "Optolink" Ltd allows fabricating fibers with following parameters:

- loss of optical light power, α — 3÷4 dB/km;
- polarization beat length, L_p — ≤2.5 mm;
- coefficient of intermode polarization coupling, h — $\leq 10^{-5}$ m^{-1};
- outer diameter, d — ≤80 μm.

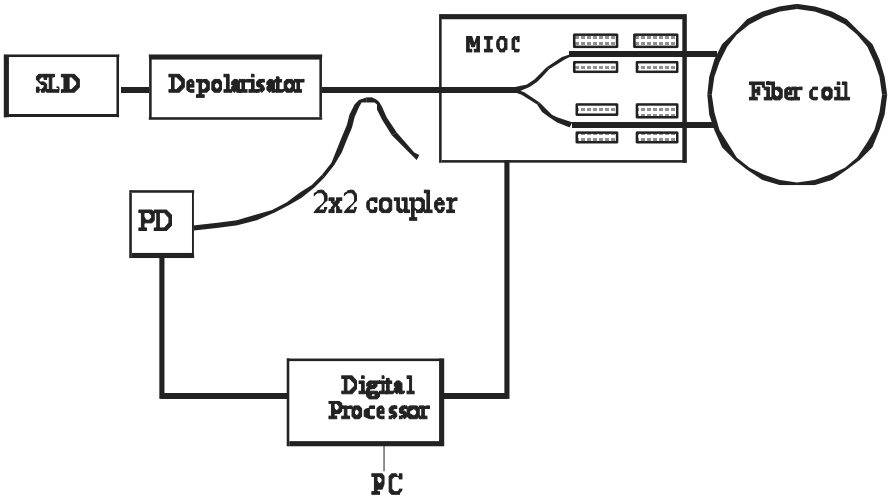

Fig.4. Fiber–optical gyroscope minimum configuration.

The light source ILPN-330-4, supplied by "Inject" Ltd., Russia is used. It contains the following components:

- Stripline superluminescent diode on the basis of double heterostructure system GaAs/GaAlAs with opposing *p-n* junction, which have an absorbe layer in the active area. Such design of superluminescent diode provides practically smooth spectrum with halfwidth 15÷18 nm and with light power up to 1,5÷2 mW on an output built - in single-mode fiber waveguide.
- Microcooler on the base of Pelletie elements for maintaining superluminescent diode crystal temperature in the given range at joint operation with the thermal control device.
- Thermoresistor for error signal formation in the thermal control device.
- The photodiode on the basis of silicon p-i-n structure for formation of a steering command in the stabilizer of power light.

All components in the ILPN -330-4 are placed in the standard hermetic case.

As a light detector the photodiode based on p-i-n of structure is used. The photodiode has electric current sensitivity to the wavelength λ = 0.835 μm not less than 0.3 A/W with delay time of a pulse signal front no more than 2 ns.

Finally, FOG with following parameters is realized:

Bias repeatability, 3σ , $^{\circ}$/h	≤ 0.1
Random walk, $^{\circ}/\sqrt{h}$	≤ 0.005
Scale factor repeatability, %	≤ 0.01

REFERENCES

1. H. Lefevre, "The Fiber – Optic Gyroscope", Artech House, 1993.
2. Y.N. Korkishko, V.A. Fedorov, and O.Y. Feoktistova, "$LiNbO_3$ optical waveguide fabrication by high-temperature proton-exchange", *IEEE J. Lightwave Technol*. **18**, pp.562-568, 2000.
3. P.G. Suchoski, T.K. Findakly, and F.J. Leonberger, "Stable low-loss proton-exchanged $LiNbO_3$ devices with no electro-optic degradation", *Opt. Lett.* **13**, pp.1050-1052, 1988.
4. Yu.N.Korkishko, V.A.Fedorov, and F.Laurell, "The SHG-Response of Different Phases in Proton Exchanged Lithium Niobate Waveguides", *IEEE J. Sel. Topics Quantum Electron*. **6**, pp.132-142, 2000.
5. K. El Hadi, M. Sundheimer, P. Aschieri, P. Baldi, M.P. De Micheli, D.B. Ostrowsky, and F. Laurell, "Quasi-phase-matched parametric interactions in proton-exchanged lithium niobate waveguides", *J. Opt. Soc. Am.* **B14**, pp.3197-3203, 1997.
6. P. Baldi, M.P. De Micheli, K. El Hadi, S. Nouh, A.C. Cino, P. Aschieri, and D.B. Ostrowsky, "Proton exchanged waveguides in $LiNbO_3$ and $LiTaO_3$ for integrated lasers and nolinear frequency converters", *Opt. Eng.* **37**, pp.1193-1202, 1998.
7. L. Chanvillard, P. Aschieri, P. Baldi, M. De Micheli, D.B. Ostrowsky, L. Huang, and D. J. Bamford, "Highly efficient integrated optical parametric generator produced by Soft Proton Exchange in PPLN", in Proceedings of the 9th European Conference on Integrated Optics (ECIO'99) (Torino, Italy, 1999), pp. 513-516.
8. J. Crank, *The mathematics of diffusion*, Clarendon, Oxford, UK, 1975.
9. Yu.N.Korkishko and V.A.Fedorov, *Ion exchange in single crystals for integrated optics and optoelectronics*, Cambridge International Science Publishing, Cambridge, UK, 1999.
10. Yu.N.Korkishko, V.A.Fedorov, E.A.Baranov, M.V.Proyaeva, T.V.Morozova, F.Caccavale, F.Segato, C.Sada, and S.M.Kostritskii, "Characterization of alpha-phase soft proton-exchanged $LiNbO_3$ optical waveguides", *J. Opt. Soc. Am.* **A18**, pp.1186-1191, 2001.
11. Yu.N.Korkishko and V.A.Fedorov, "Relationship Between Refractive Indices and Hydrogen Concentration in Proton-Exchanged $LiNbO_3$ Waveguides", *J. Appl. Phys.*, **82**, pp.171-183, 1997.
12. R.Scarmozzino, A.Gopinath, R.Pregla, and S.Helfert, "Numerical Techniques for Modeling Guided-Wave Photonic Devices", *IEEE J. Sel. Topics Quantum Electron.*, **6**, pp.150-162, 2000.